

Direct Observation of Field-Induced Incommensurate Fluctuations in a One-Dimensional S=1/2 Antiferromagnet

D. C. Dender¹, P. R. Hammar¹, Daniel H. Reich¹, C. Broholm^{1,2}, and G. Aeppli³

¹*Department of Physics and Astronomy, The Johns Hopkins University, Baltimore, Maryland*

21218

²*National Institute of Standards and Technology, Gaithersburg, Maryland 20899*

³*NEC Research Institute, 4 Independence Way, Princeton, New Jersey 08540*

(October 23, 2018)

Abstract

Neutron scattering from copper benzoate, $\text{Cu}(\text{C}_6\text{D}_5\text{COO})_2 \cdot 3\text{D}_2\text{O}$, provides the first direct experimental evidence for field-dependent incommensurate low energy modes in a one-dimensional spin $S = 1/2$ antiferromagnet. Soft modes occur for wavevectors $\tilde{q} = \pi \pm \delta\tilde{q}(H)$ where $\delta\tilde{q}(H) \approx 2\pi M(H)/g\mu_B$ as predicted by Bethe ansatz and spinon descriptions of the $S = 1/2$ chain. Unexpected was a field-induced energy gap $\Delta(H) \propto H^\alpha$, where $\alpha = 0.65(3)$ as determined from specific heat measurements. At $H = 7 \text{ T}$ ($g\mu_B H/J = 0.52$), the magnitude of the gap varies from $0.06 - 0.3J$ depending on the orientation of the applied field.

75.10.Jm, 75.25.+2, 75.50.Ee

When a conventional antiferromagnet is subject to a magnetic field the antiferromagnetically aligned spins reorient perpendicular to the field in a so-called spin flop transition, and magnetization develops through homogeneous canting of the spins in the direction of the field. A different scenario is expected for a spin $S = 1/2$ one-dimensional antiferromagnet [1–3], where the magnetization is associated with defects in the cooperative spin-singlet ground state. The effect is accounted for by mapping the spin chain to a one-dimensional system of interacting fermions [4], popularly referred to as spinons. The magnetic field causes a Zeeman splitting of the half-filled, doubly degenerate spinon band [Fig. 1(a)], and the spin chain develops soft modes [Fig. 1(b)] at the incommensurate wavevectors which connect the field-dependent Fermi points. The new periodicity, given to lowest order by the ratio of the magnetic field to the spinon velocity, coincides with the average separation between the magnetization-carrying defects. While incommensurate spin correlations do not occur in classical one-dimensional spin systems such as TMMC [5], they may be a general feature of one-dimensional quantum spin chains [3,6]. In this letter we present the first direct experimental evidence for incommensurate spin fluctuations in a uniform antiferromagnetic $S = 1/2$ chain.

To search for incommensurate spin correlations, we used inelastic neutron scattering to probe the wavevector-dependent spin susceptibility of the model one-dimensional $S = 1/2$ antiferromagnet (AFM) copper benzoate, $\text{Cu}(\text{C}_6\text{D}_5\text{COO})_2 \cdot 3\text{D}_2\text{O}$. In contrast to other systems that have been studied in this context [7,8], in copper benzoate the exchange constant J is small enough to permit the large values of the reduced field, $h = g\mu_B H/J \approx 1$ needed to observe this effect, while still being large enough to allow the interesting low energy part of the spectrum to be explored with a cold neutron triple-axis spectrometer [9]. Our most important result is that a magnetic field induces new low-energy modes in the excitation spectrum of copper benzoate at incommensurate wavevectors $\tilde{q} = \pi \pm \delta\tilde{q}$, where $\delta\tilde{q}(H) \approx 2\pi M(H)/g\mu_B$, with $M(H)$ being the magnetization per spin, as predicted by theory [1–3]. The modes are not completely soft, however, because the field also induces a gap in the excitation spectrum both at the incommensurate wave vector and at $\tilde{q} = \pi$.

First identified as a linear chain AFM by Date *et al.* [10], copper benzoate is centered monoclinic, space group $I2/c$, with room temperature lattice constants $a = 6.98 \text{ \AA}$, $b = 34.12 \text{ \AA}$, $c = 6.30 \text{ \AA}$, and $\beta = 89.5^\circ$ [11]. Copper ions within a spin chain are separated by $\mathbf{c}/2$ and coordinated by edge sharing, tetragonally distorted oxygen octahedra. The near-neighbor intrachain exchange interaction is $J = 1.57 \text{ meV}$ [9]. For this work, deuterated single crystals were prepared as described previously [9]. Specific heat measurements in magnetic fields up to $H = 8.8 \text{ T}$ were made on individual single crystals of typical mass 0.01 g using the relaxation method. For the neutron scattering measurements, approximately 500 crystals with total mass 3.82 g were mutually aligned to within 5° in the horizontal ($h0l$) scattering plane. Neutron scattering measurements in fields up to $H = 7 \text{ T} \parallel \hat{\mathbf{b}}$ were performed on the SPINS cold neutron triple-axis spectrometer at NIST. FWHM beam divergences were $50'/k_i(\text{\AA}^{-1}) - 80' - 80' - 215'$, and the fixed final energy was 2.5 meV , yielding energy and wavevector resolution $\Delta E = 69 \text{ } \mu\text{eV}$ and $\Delta\tilde{q}/\pi = 0.02$, respectively. We refer to wave vector transfer along the chain as $\tilde{q} = \mathbf{Q} \cdot \mathbf{c}/2 = l\pi$. The normalized magnetic scattering intensity $\tilde{I}(\tilde{q}, \omega)$ [9], was derived from the detector count rate by subtracting $T = 25 \text{ K}$ data as a background, dividing by the squared magnetic form factor for copper, and normalizing to incoherent elastic scattering from vanadium.

Figure 2 shows the \tilde{q} -dependence of the low energy ($\hbar\omega = 0.21 \text{ meV}$) and low temperature ($T = 0.3 \text{ K}$) inelastic magnetic neutron scattering intensity from copper benzoate for four values of H . At $H = 0$ there is a single peak centered at $\tilde{q} = \pi$. This peak is much broader than the instrumental resolution $\Delta\tilde{q}$, and arises when $\hbar\omega$ and \tilde{q} lie within the two-spinon continuum of the $S = 1/2$ AFM chain [3,9,13,14]. In finite field, the data show additional peaks at incommensurate values of wave vector transfer, $\pi \pm \delta\tilde{q}$, where $\delta\tilde{q}$ increases with H . The data of Fig. 2 represent the first direct experimental observation of a field-induced incommensurate length scale in a uniform spin-1/2 chain and is the central result of this paper.

To extract the field dependence of the wavevector $\delta\tilde{q}$ for quantitative comparison to theory, one needs a specification of the full \tilde{q} - and $\hbar\omega$ -dependent magnetic density of states.

Toward this end, we have performed both specific heat measurements, which are sensitive to the momentum space average of the density of states, and constant- \tilde{q} neutron scattering scans at $\tilde{q} = \pi$ and at $\tilde{q} = 1.12\pi$, which is the wavevector at which the incommensurate peak occurs at $H = 7$ T. Figure 3 shows the resulting neutron scattering data. In zero field at $\tilde{q} = \pi$ [Fig. 3(a)], the threshold for magnetic scattering is $\hbar\omega \approx 0$, and the intensity decreases monotonically for $\hbar\omega > 0$. At $\tilde{q} = 1.12\pi$ [Fig. 3(b)], the threshold has increased to $\hbar\omega \approx 0.8$ meV, with no magnetic scattering visible below that energy. The lines through the data in the bottom two frames of Fig. 3 were calculated by convolving the zero-field dynamic spin correlation function derived by Schulz [15] with the instrumental resolution.

The spectrum changes dramatically for $H = 7$ T, as shown in Fig. 3(c) and Fig. 3(d). At $\tilde{q} = \pi$, there is no magnetic scattering for $\hbar\omega < 0.1$ meV, indicating that a gap has developed in the spectrum. Above this gap, a sharp, resolution-limited mode peaked at $\hbar\omega = 0.17$ meV now marks the onset of the continuum. A second, resolution-limited mode also appears at $\tilde{q} = \pi$ at an energy close to the Zeeman energy $g\mu_B H = 0.81$ meV. Figure 3(b) reveals that at $H = 7$ T, the spectrum at the incommensurate wave vector $\tilde{q} = 1.12\pi$ also has a gap to a resonant mode at $\hbar\omega = 0.22$ meV. The dependence of the intensity of the resonant modes on the angle between the total wavevector transfer \mathbf{Q} and the chain axis is consistent with the theoretical expectation [3] that the incommensurate mode is polarized parallel to the field, and the mode at $\tilde{q} = \pi$ is polarized perpendicular to it [16].

We now turn to the specific heat measurements, which explore the field dependence of the gap. Figure 4 shows specific heat data for copper benzoate for the same values and orientation of the applied field ($H \parallel \hat{\mathbf{b}}$) as for the data in Fig. 2. The total specific heat for $H = 0$ and 3.5 T is shown in the inset, plotted as C_{tot}/T . A small lattice contribution to C_{tot} below $T = 1$ K is visible in the slight temperature dependence of C_{tot}/T for $H = 0$. Fitting the $T < 1$ K zero-field data to $C_{tot}/T = a + bT^2$ gives $b = 0.024(5)$ J/mol K⁴. This lattice term was subtracted from all the data, and the main part of Fig. 4 shows the resulting magnetic specific heat C . The linear magnetic specific heat we observe in zero field is consistent with the low-energy linear dispersion relation of the spinons in the 1D

spin-1/2 AFM. The fit shown gives $C(T) = 0.68(1)R(k_B T/J)$, in excellent agreement with the theoretical value of $C(T) = 0.7R(k_B T/J)$ [17]. The data set an upper limit of $\approx 9 \mu\text{eV}$ for any zero-field gap and an upper limit $\Delta S < 3 \times 10^{-3}R \ln 2$ on the entropy change of any magnetic phase transition for $T > 0.1 \text{ K}$ [18].

In finite fields and at low T , C is suppressed below its zero field value. As T increases, $C(H, T)$ rises above the zero-field curve, before settling back down to it at high T (inset to Fig. 4). This behavior indicates a transfer of spectral weight from low to higher energies, and is a clear signature of a field-induced gap $\Delta(H)$.

To determine the field dependence of Δ , we fit the $H \neq 0$ data in Fig. 4 to

$$C = \frac{\tilde{n}R}{\sqrt{2\pi}} \left(\frac{\Delta}{k_B T} \right)^{3/2} \frac{\Delta}{v} \exp(-\Delta/k_B T), \quad (1)$$

which is the low- T specific heat [19] for \tilde{n} species of non-interacting one-dimensional bosons with a gap and dispersion relation

$$\hbar\omega(\tilde{q}) = \sqrt{\Delta^2 + (v(\tilde{q} - \tilde{q}_0))^2}, \quad (2)$$

A term proportional to H^2/T^2 was included in the fit to take into account the small nuclear spin contribution. The fits are shown as solid lines in Fig. 4, and Fig. 5(b) summarizes the field dependence of the gaps derived from this analysis as well as for data we have taken with H along the other principal magnetic directions, \mathbf{c}'' and \mathbf{a}'' [12]. The average of the gaps measured by neutron scattering for $H = 7 \text{ T} \parallel \hat{\mathbf{b}}$, at $\tilde{q} = \pi$ and 1.12π (filled symbols in Fig. 5(b)) correspond nicely to the gap derived from specific heat. Moreover the values of $v/\tilde{n} = 0.49(3)$, $0.55(3)$, and $0.96(5)$ meV/mode for $H \parallel \mathbf{b}$, \mathbf{c}'' and \mathbf{a}'' , respectively, are not far from the crude estimate $v/\tilde{n} \approx 0.5\pi J/6 = 0.41$ meV/mode, where $\tilde{n} = 6$ is the number of soft modes in a Brillouin zone. The field dependence of the gaps is described by the power-law $\Delta(H) = AH^\alpha$ with $\alpha = 0.65(3)$. The prefactors A are in ratios $1 : 2.0 : 0.55$ for H applied along the \mathbf{b} , \mathbf{c}'' and \mathbf{a}'' directions, respectively. A slightly better fit to the \mathbf{c}'' data is obtained by including a finite critical field: $\Delta(H) = A(H - H_c)^\alpha$, where $H_c = 0.25(3) \text{ T}$ and $\alpha = 0.58(3)$. We note that small field-dependent gaps are not found in the classical easy

plane AFM spin chain TMMC, where a field in the easy plane induces a central diffusive soliton mode and a gap $\Delta(H) = g\mu_B H$ [5,20].

With the information about the field-dependence of the gap derived from the specific heat data, we can extract the field-dependent incommensurate wave vector from the neutron scattering data in Fig. 2. We approximate the low energy response as resonant modes with dispersion relations given by Eq. (2), where $\tilde{q}_0 = \pi$ or $\pi \pm \delta\tilde{q}(H)$ (see Fig. 1(b)). The velocity v was fixed at the zero field value $\pi J/2$ [21], and the gap $\Delta(H)$ was taken from the specific heat measurements. Although it neglects the continuum scattering above the resonant modes that is visible in Figs. 3(a) and 3(b), this model provides a reasonable fit for the finite field constant- $\hbar\omega$ scans in Fig. 2. Note that for $H = 3.5$ T, it appears that a single branch of the dispersion relation at the incommensurate wave vector is resolved, while the other merges into a broad central peak at $\tilde{q} = \pi$. Thus the incommensurate wavevector at this field actually lies at the local minimum between the peaks. This is in contrast to the $H = 5$ T and $H = 7$ T data, where the incommensurate modes are well-separated from the $\tilde{q} = \pi$ mode, and the energy of the scan is very close to the gap. The fits establish that the incommensurate peaks are resolution-limited, and also provide a systematic way of deriving the field-dependent incommensurate wavevector $\delta\tilde{q}(H)$. This is shown as a function of H in Fig. 5(a). The solid line in this figure is the theoretical prediction [3]: $\delta\tilde{q}(H) = 2\pi M(H)/g_b\mu_B$ with $g_b = 2.06$ [12]. $M(H)$ is calculated using Eq. (2.24) of Ref. [3], which provides an excellent description of the magnetization for copper benzoate [22]. Despite the complications associated with the field-induced gaps, the theory accounts well for the field-dependent positions of the incommensurate soft modes.

In summary we have provided the first direct experimental evidence for field-dependent incommensurate soft modes in a $S=1/2$ one dimensional antiferromagnet. Thus, one of the key features of the spinon description of $S=1/2$ AFM chains, namely a chemical potential which can be regulated by an external field, has finally been verified. Our results also have implications beyond the nearest-neighbor coupled $S=1/2$ chain. For example, theoretical studies predict that both long-range coupled models [23] and systems such as ladders

and dimerized chains with intrinsic gaps [6] should show similar behavior, indicating that field-induced incommensurabilities are a general property of quantum spin chains. The incommensurate lattice distortions recently observed in TTF-CuBDT [24] and CuGeO₃ [25] may therefore be closely related to our results. In copper benzoate, the field also introduces gaps in the excitation spectrum both at the commensurate and at the incommensurate wave vector, something which was not predicted by theories for isotropic Heisenberg spin chains. Possible causes for the gaps are diagonal as well as off-diagonal exchange anisotropies, and a staggered g-factor anisotropy [12] which induces a small effective staggered field when a homogeneous external field is applied .

We are grateful for discussions with A. Millis, and for the hospitality of K. Clausen at Risø National Laboratory, where preliminary data were collected. NSF grants DMR-9302065, and DMR-9453362 supported work at JHU. This work utilized neutron research facilities supported by NIST and the NSF under Agreement No. DMR-9423101. DHR acknowledges support from the David and Lucile Packard Foundation.

REFERENCES

- [1] E. Pytte, Phys. Rev. **10**, 4637 (1974).
- [2] N. Ishimura and H. Shiba, Prog. Theor. Phys. Jpn. **57**, 6 (1977); **57**, 1862 (1977); **64**, 479 (1980).
- [3] G. Müller *et al.*, Phys. Rev. B **24**, 1429 (1981).
- [4] G. Baskaran, Z. Zou, and P. W. Anderson, Solid State Commun. **63**, 973 (1987); D. P. Arovas and A. Auerbach, Phys. Rev. B **38**, 316 (1988).
- [5] L. P. Regnault *et al.*, J. Phys. C, **15**, 1261 (1982).
- [6] R. Chitra and T. Giamarchi, Phys. Rev B **55**, 5816 (1997).
- [7] I. U. Heilmann *et al.*, Phys. Rev. B **18**, 3530 (1978).
- [8] R. Coldea, D. A. Tennant, R. A. Cowley, D. F. McMorrow, B. Dorner, and Z. Tylczynski, preprint, (1997).
- [9] D. C. Dender *et al.*, Phys. Rev. B **53**, 2583 (1996).
- [10] M. Date *et al.*, Suppl. Prog. Theor. Phys. **46**, 194 (1970).
- [11] H. Koizumi, K. Osaki, and T. Watanabé, J. Phys. Soc. Japan **18**, 117 (1963).
- [12] K. Okuda, H. Hata, and M. Date, J. Phys. Soc. Japan **33**, 1574 (1972); K. Oshima, K. Okuda, and M. Date, *ibid.* **41**, 475 (1976); **44**, 757 (1978); K. Nagata and K. Okuda, *ibid.* **46**, 1726 (1979). K. T. McGregor and Z. G. Soos, J. Chem. Phys. **64**, 2506 (1976).
- [13] A. H. Bougourzi, M. Couture, and M. Kacir, Phys. Rev. B **54**, R12669 (1996); M. Karbach, G. Müller, and A. H. Bougourzi, Preprint cond-mat/9606068.
- [14] D. A. Tennant *et al.*, Phys. Rev. Lett. **70**, 4003 (1993).
- [15] H. J. Schulz, Phys. Rev. B **34**, 6372 (1986).

- [16] D. C. Dender *et al.*, unpublished. At $H = 7$ T and $\hbar\omega = 0.21$ meV, the incommensurate resonant mode's angular dependence in the $(h, 0, l)$ plane is completely accounted for by the Cu form factor, while the $\tilde{q} = \pi$ mode is found to contain only spin fluctuations $\perp H$ and $\parallel \mathbf{a}''$.
- [17] J. C. Bonner and M. E. Fisher, Phys. Rev. **135**, A640 (1964)
- [18] K. Takeda *et al.*, J. Phys. Soc. Japan, **49**, 162 (1980).
- [19] M. Troyer, H. Tsunetsugu, and D. Würtz, Phys. Rev. B **50**, 13515 (1994).
- [20] I. U. Heilmann *et al.*, Phys. Rev. B **24**, 3939 (1981).
- [21] J. des Cloizeaux and J. J. Pearson, Phys. Rev. **128**, 2131 (1962).
- [22] T. Yosida, in "High Field Magnetism," M. Date, ed., (North Holland, 1983), p. 305.
- [23] J. C. Talstra, and F. D. M. Haldane, Phys. Rev. B **50**, 6889 (1994).
- [24] V. Kiryukhin, B. Keimer, and D. E. Moncton, Phys. Rev. Lett. **74**, 1669 (1995).
- [25] V. Kiryukhin *et al.*, Phys. Rev. Lett. **76**, 4608 (1996).

FIGURES

FIG. 1. (a) Schematic of the Zeeman-split bands of the fermion mean field theory for the $S=1/2$ AFM chain in a magnetic field H . The Fermi energy is at $E = 0$. Solid (dashed) arrows show incommensurate (commensurate) spanning vectors. (b) Boundaries of the resulting spinon continua, for spin fluctuations parallel (solid lines) and perpendicular (dashed lines) to H . Note incommensurate soft modes near $\tilde{q} = \pi$. Horizontal dotted line shows trajectory of scans in Fig. 2.

FIG. 2. Magnetic scattering at $\hbar\omega = 0.21$ meV along the $(0.3,0,l)$ direction for four values of magnetic field H at $T = 0.3$ K. The solid lines for $H \neq 0$ are fits to resolution-limited spin wave scattering as described in the text. The line through the $H = 0$ T data is the theory [15] for the dynamic spin correlation function convolved with the experimental resolution. A correction factor varying from 0.7 to 0.95 over the range of the scan was applied to the model to take into account the measured \tilde{q} dependent sample transmission.

FIG. 3. Energy dependence of the magnetic scattering intensity at $T = 0.3$ K for $\mathbf{Q} = (0.3, 0, 1)$ and $\mathbf{Q} = (0.3, 0, 1.12)$ at $T = 0.3$ K. The latter wave vector corresponds to the position of the incommensurate maxima in the $H = 7$ T constant- $\hbar\omega = 0.21$ meV scan. The solid lines through the $H = 0$ T data are the theoretical dynamic correlation function [15] convolved with the experimental resolution. The dashed lines are the average of the data in (b) for 0.08 meV $< \hbar\omega < 0.6$ meV, which is a good measure of the over-subtraction caused by isotropic magnetic scattering contained in the $T = 25$ K data used as a background.

FIG. 4. Specific heat of copper benzoate as a function of temperature for four values of applied field $H \parallel \hat{\mathbf{b}}$. Inset: total specific heat plotted as C_{tot}/T for $H = 0$ and 3.5 T. Main panel: magnetic heat capacity C after subtraction of phonon contribution. Solid lines are from fits described in the text.

FIG. 5. (a) Field dependence of the displacement $\delta\tilde{q}$ of the incommensurate side peaks from $\tilde{q} = \pi$ in copper benzoate, as derived from fits to the data shown in Fig. 2. The solid line is the theoretical curve from Ref. [3]. (b) Field dependence of the energy gap derived from fits to specific heat data such as those shown in Fig. 4. Data for fields along the three principal magnetic directions are shown. Filled symbols are the gaps measured at $\tilde{q} = \pi$ and $\tilde{q} = 1.12\pi$ by neutron scattering. The solid lines are from fits to power-laws described in the text.

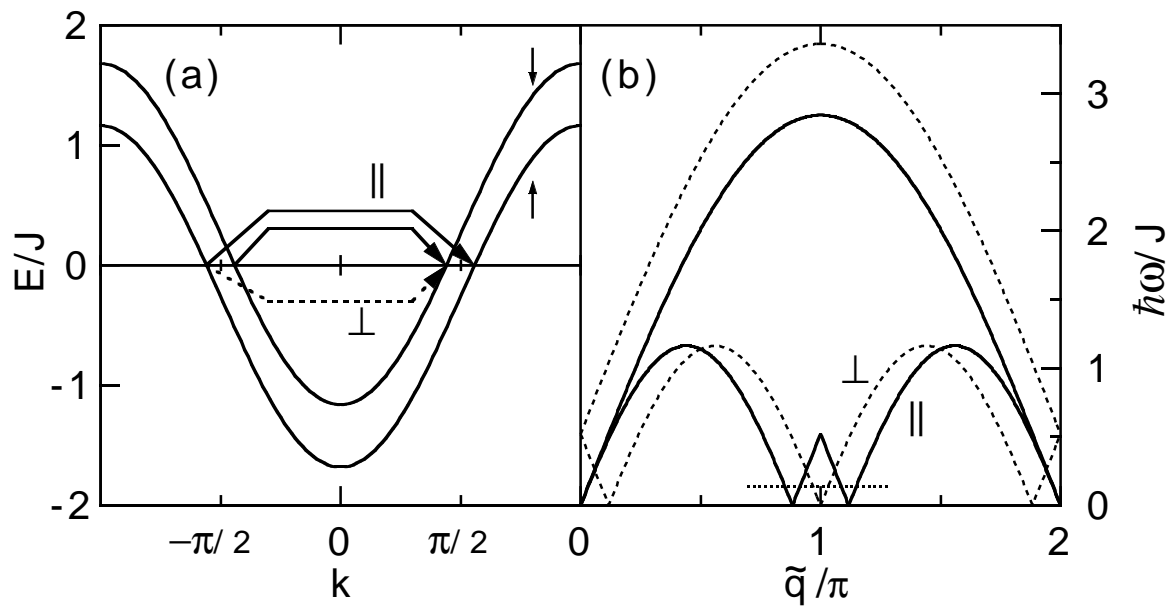


Fig. 1 Dender et al.

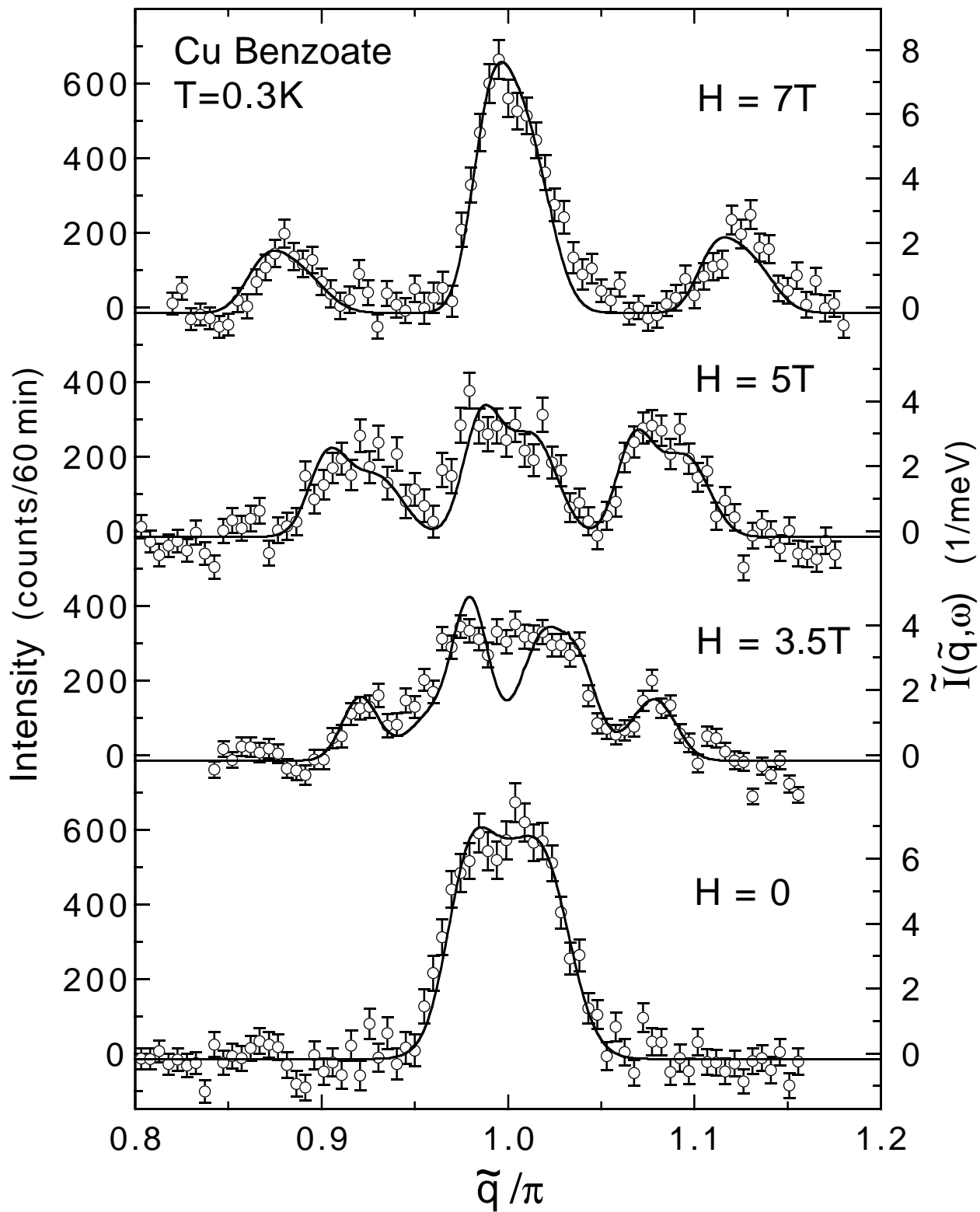


Figure 2. Dender et al.

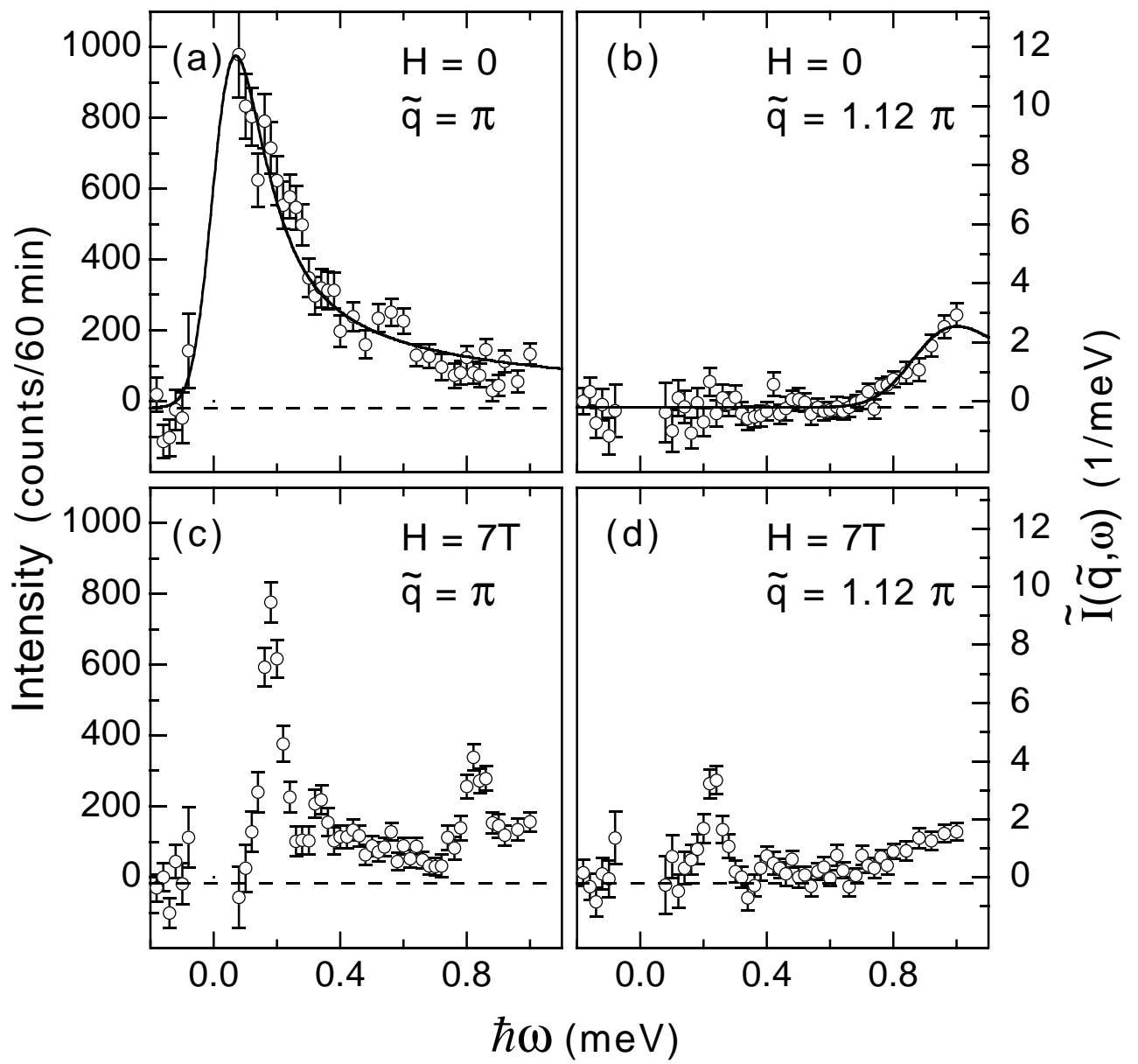


Figure 3. Dender et al.

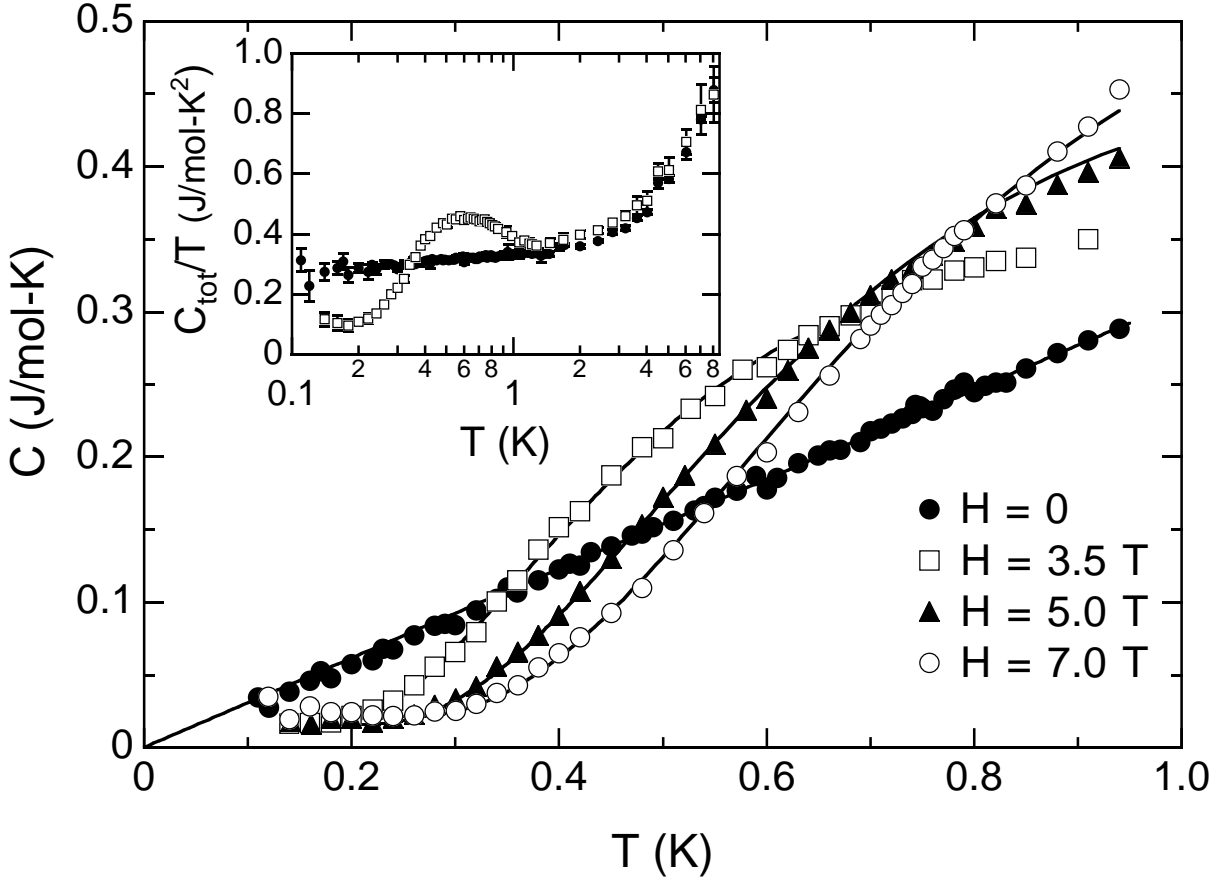


Fig. 4, Dender, et al.

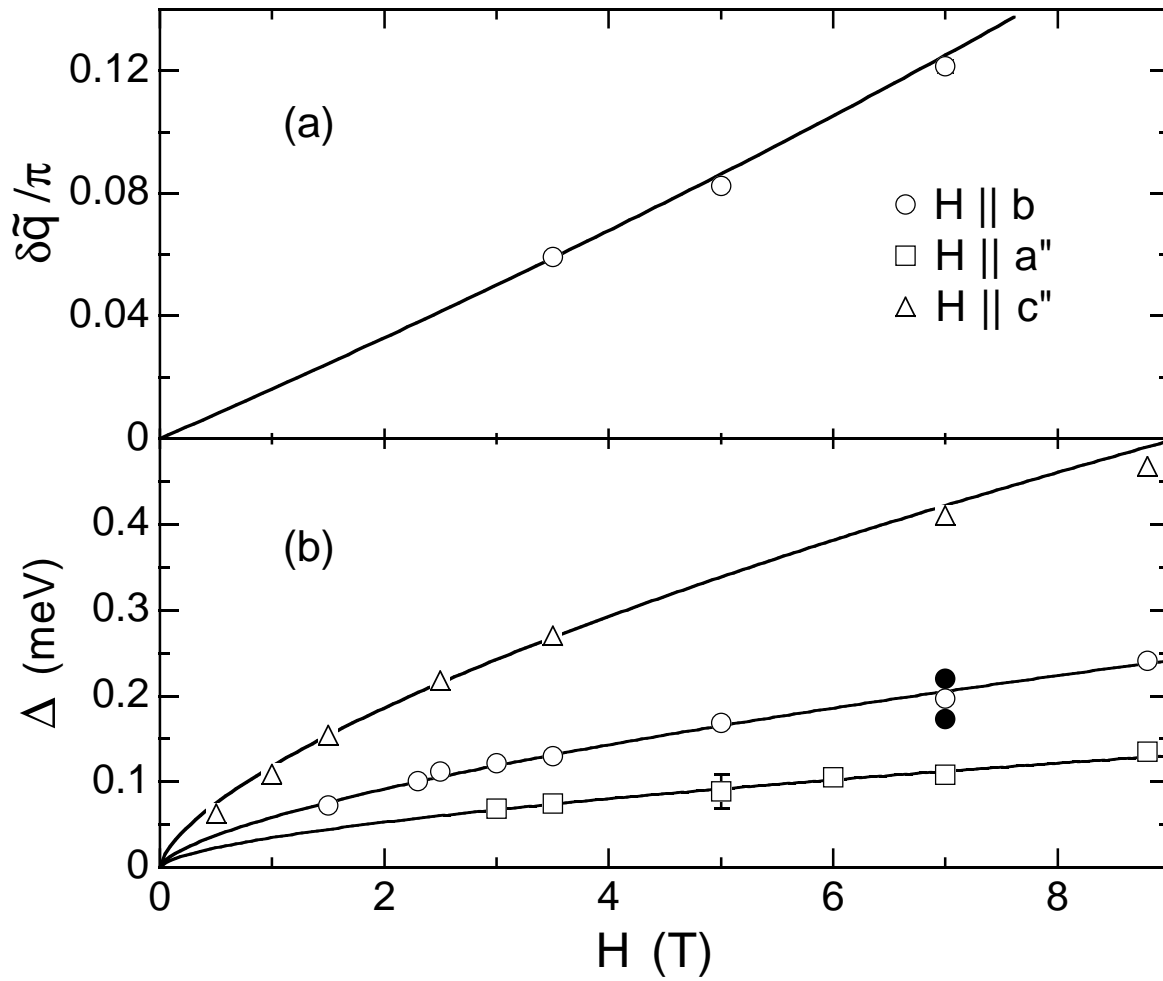


Fig. 5 Dender, et al.